Supporting Information

Supporting Data

Fig. S1

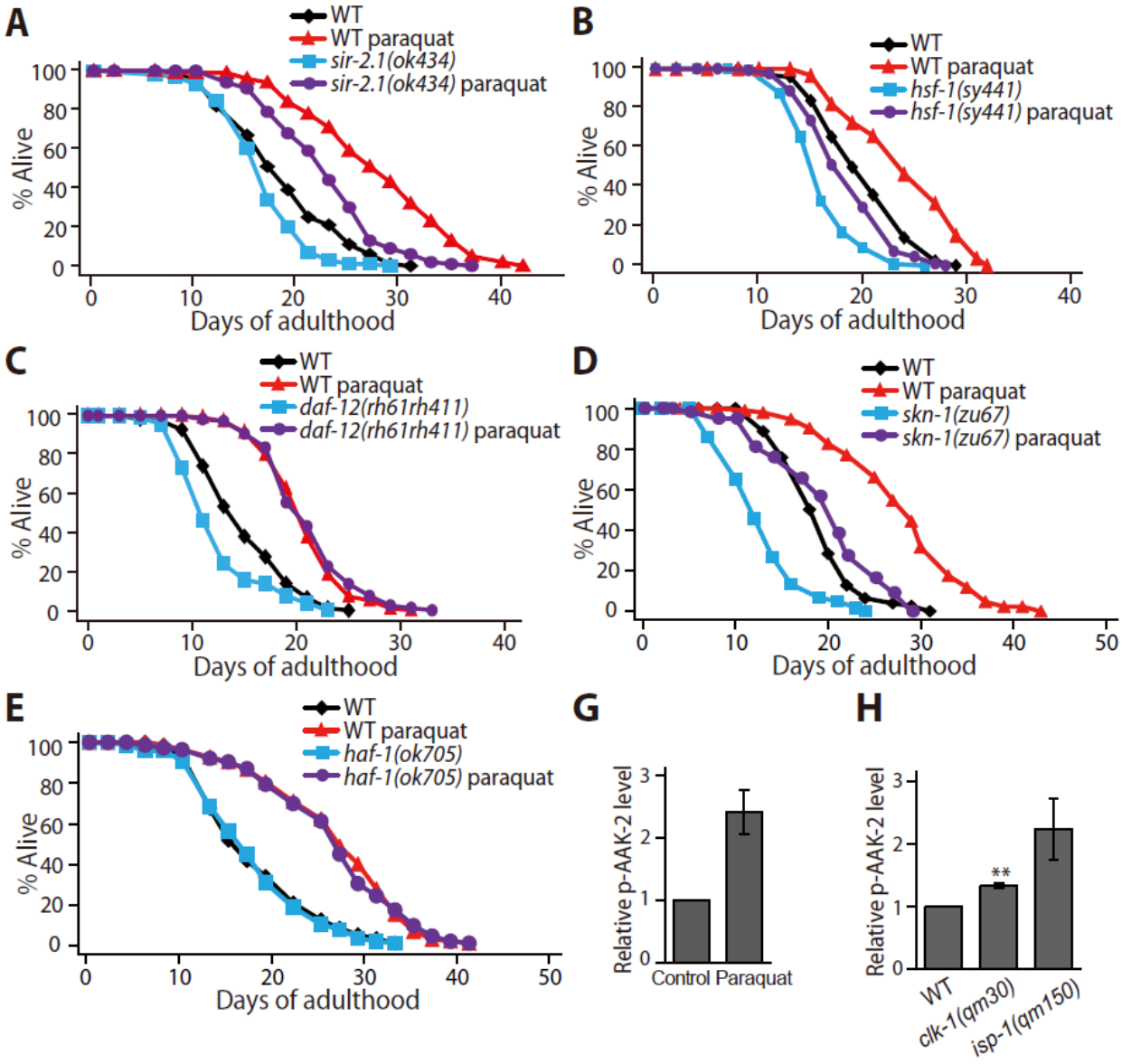

Fig. S1. The effect of paraquat (0.25 mM) treatment on the lifespan of various mutants defective in lifespan-regulatory genes. The longevity induced by 0.25 mM paraquat treatment

was not suppressed by mutations in NAD-dependent protein deacetylase/*sir-2.1(ok434)* (**A**), heat shock transcription factor 1/*hsf-1(sy441)* (**B**), nuclear receptor *daf-12(rh61rh411)* (**C**), NRF2-related transcription factor/*skn-1(zu67)* (**D**), or mitochondrial ABC transporter/*haf-1(ok705)* (**E**). The *hsf-1*- and *skn-1*-independent longevity caused by paraquat treatment is consistent with the observations in a previous study (1). See **Table S1** for statistical analysis and additional repeats. (**G-H**) The bar graphs are the quantification of the p-AAK-2 band intensity of Western blot data from **Figures 1G** (n=4, p=0.052) (**G**) and **1H** (n=3, p=0.062 for *isp-1* mutants) **(H)**. Error bars represent SEM (**p<0.01, Student's *t*-test).

Fig. S2

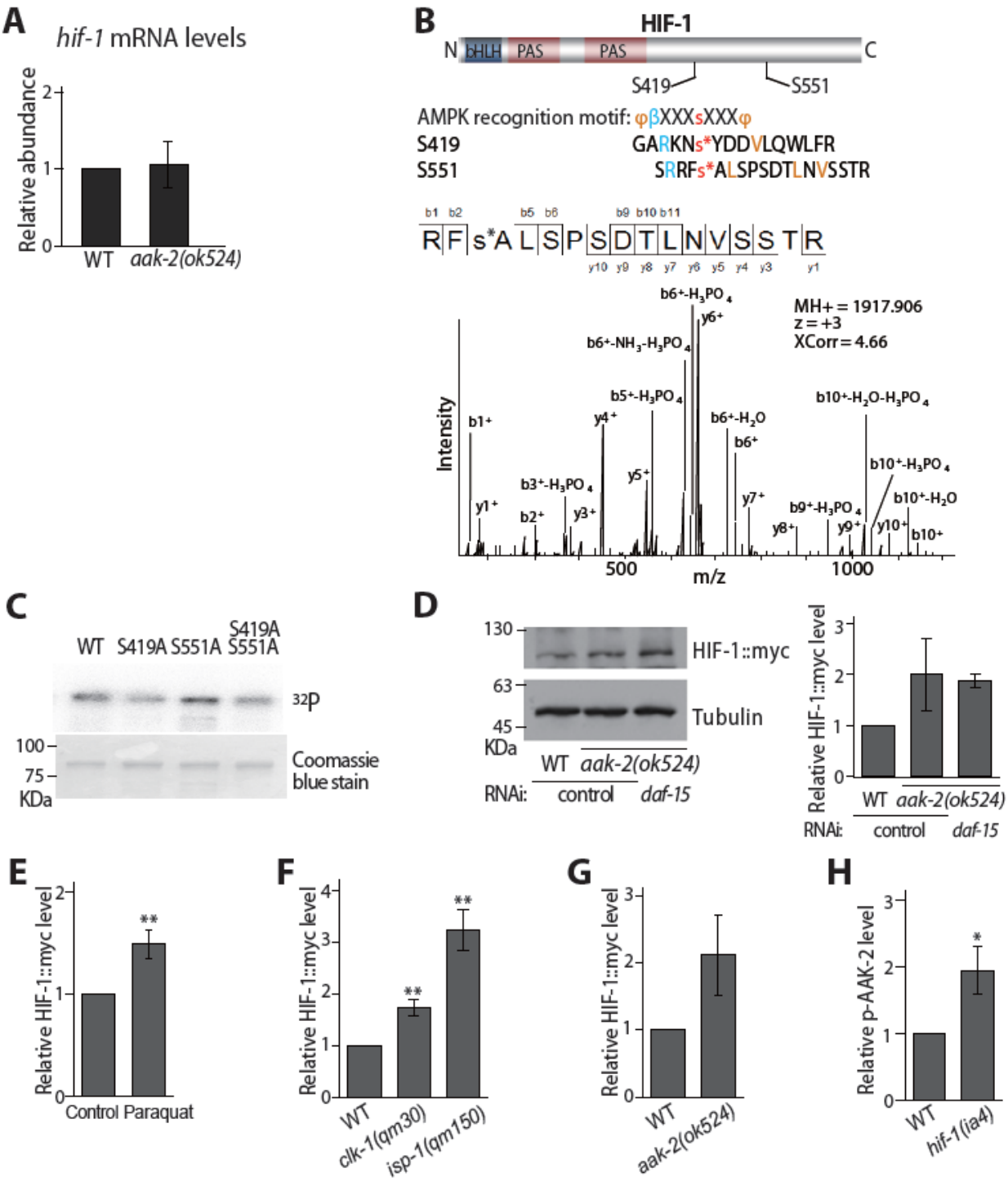

Fig. S2. Regulation of HIF-1 by AAK-2 via phosphorylation. (**A**) The mRNA levels of *hif-1*

measured by using quantitative reverse transcriptase-polymerase chain reaction (qRT-PCR) were not changed by *aak-2(ok524)* mutations (n=6). (**B**) MS/MS spectrum recorded using a Q Exactive mass spectrometer for the triply charged peptide RFs*ALSPSDTLNVSSTR (MH+ = 1917.90635, z = +3, XCorr = 4.66). The peptide contains the S551 phosphorylation site. Daughter ions are annotated according to the nomenclature for peptide fragmentation in mass spectrometry. (**C**) In addition to S419 (**Figure 2E**), mass spectrometry analysis identified S551 as another potential phosphorylation site, which is modestly conserved with AMPK recognition motif. However, different from S419A mutation, S551A mutation did not reduce the level of phospho-GST-HIF-1C. The reduced phospho-HIF-1 level of S419A S551A mutant was similar to that of S419A. bHLH, basic helix-loop-helix domain; PAS, PER-ARNT-SIM domain; φ, hydrophobic residues; β, basic residues. Coomassie blue staining showed total protein load. (**D**) AMPK may down-regulate TOR (target of rapamycin), another key cellular energy sensor, which increases HIF-1 translation, as shown in mammalian cells (2, 3). However, knockdown of *daf-15/Raptor* did not influence the increased level of HIF-1::myc in *aak-2* mutants. The bar graph is the quantification data of the relative band intensity of HIF-1::myc levels normalized to tubulin (n=2). Transgenic animals expressing HIF-1::myc in wild-type or *aak-2* mutant background were treated with control or *daf-15* RNAi, which was retrieved from the Julie Ahringer *C. elegans* RNAi library, for 3 days with FUDR. α-tubulin was used as a loading control. (**E**-**H**) The quantification data of Western blot band intensity. The bar graph indicates relative HIF-1::myc levels from **Figures 2A** (n=5) (**E**), **2B** (n=4) (**F**), and **2C** (n=6, p=0.093) (**G**), and the relative phospho-AAK-2 levels from **Figure 2H** (n=4) (**H**). *aak-2* was not included in the genes whose expression levels were differentially regulated by hypoxia in previous microarray data (4). In another microarray analysis, the expression of *aak-2* was increased by 1.62 fold (n=1) in *vhl-1*

mutants (5). Further experiments are required in the future to determine whether HIF-1 affects AMPK directly or indirectly in various conditions. Error bars represent SEM (*$p<0.05$, **$p<0.01$, Student's *t*-test).

Fig. S3

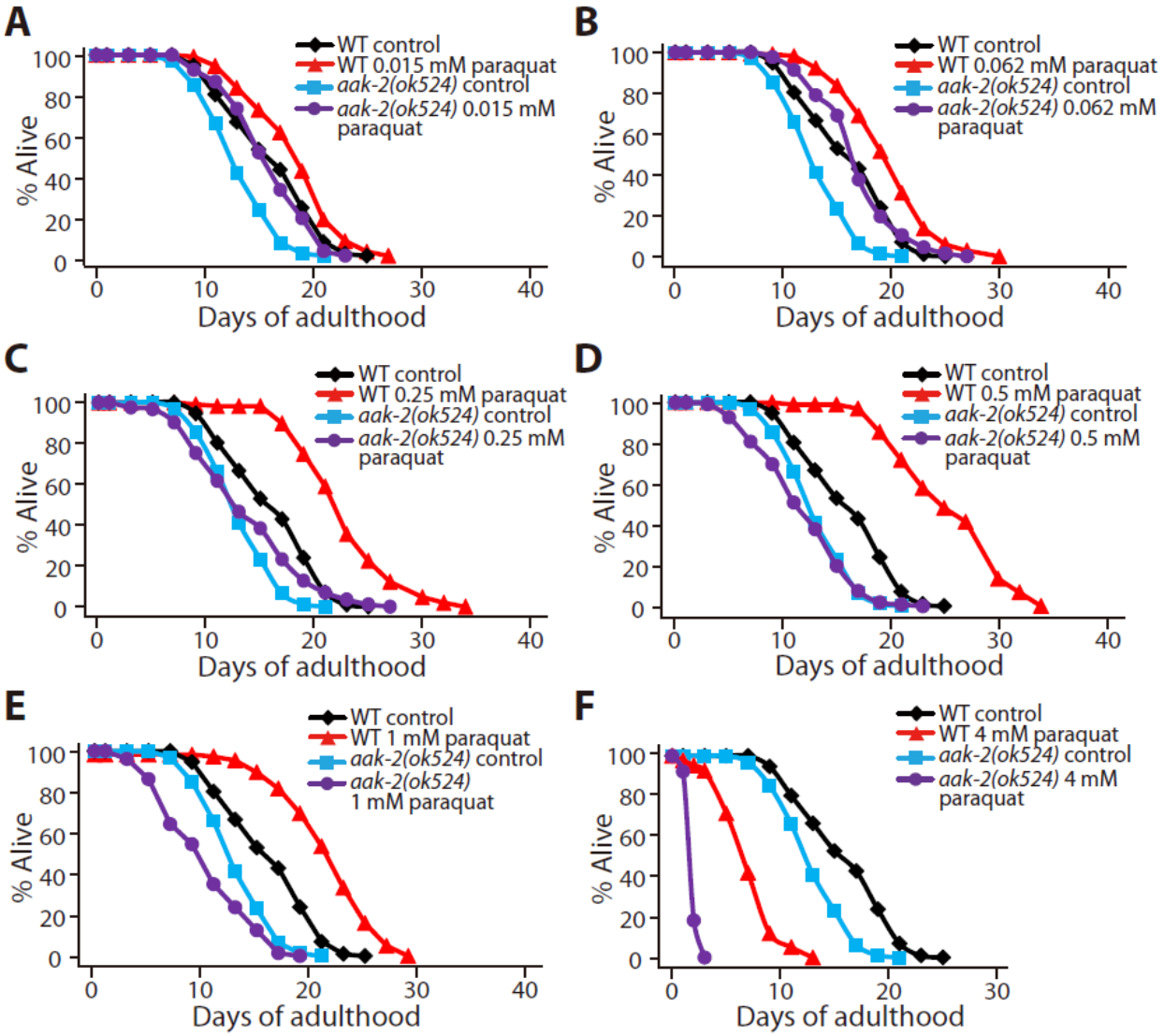

Fig. S3. The lifespan of *aak-2* mutants treated with various doses of paraquat.

Representative lifespan curves of wild-type and *aak-2(ok524)* animals with or without various concentrations of paraquat, 0.015 mM (**A**), 0.062 mM (**B**), 0.25 mM (**C**), 0.5 mM (**D**), 1 mM (**E**), and 4 mM (**F**) during adulthood. Yang and Hekimi reported that 0.1 mM paraquat treatment increased the lifespan of *aak-2* mutants (1), which, at first glance, appears different from our results. However, these data are actually consistent with one another because we showed that

aak-2 mutants lived longer at lower concentrations of paraquat (**A** and **B**) while not surviving long at the higher concentrations (**C** or **D**) that increased wild-type lifespan. Curtis et al. reported that the *aak-2* mutations partially suppress longevity in *clk-1* and *isp-1* mutants (6). Because we found that *aak-2* mutations further increased ROS levels in *isp-1* mutants (**Figure 3F**), we speculate that *aak-2* mutations increase internal ROS levels in the respiration mutants to a toxic level that decreases longevity. However, two recent reports showed that AMPK is required for the generation of ROS in *C. elegans* (7, 8), which seems to conflict with our data. One noticeable difference was that the other two reports showed that *aak-2* mutations decreased ROS levels in animals with reduced insulin/IGF-1 signaling (IIS). Thus, the role of AMPK in ROS regulation is different in animals with reduced IIS compared to that in animals that have defective mitochondrial respiration. Interestingly, the longevity of IIS mutants is associated with an up-regulation of genes that detoxify ROS (9-11), whereas the increased lifespan of mitochondrial respiration mutants is linked to increased ROS levels (1, 12). Because reduced IIS and elevated mitochondrial ROS lengthen lifespan at least partially through AMPK (6, 13; this study), it is likely that AMPK contributes to the longevity of IIS and mitochondrial respiration mutants by balancing the levels of ROS in a context-dependent manner. See **Table S2** for statistical analysis and additional repeats.

Fig. S4

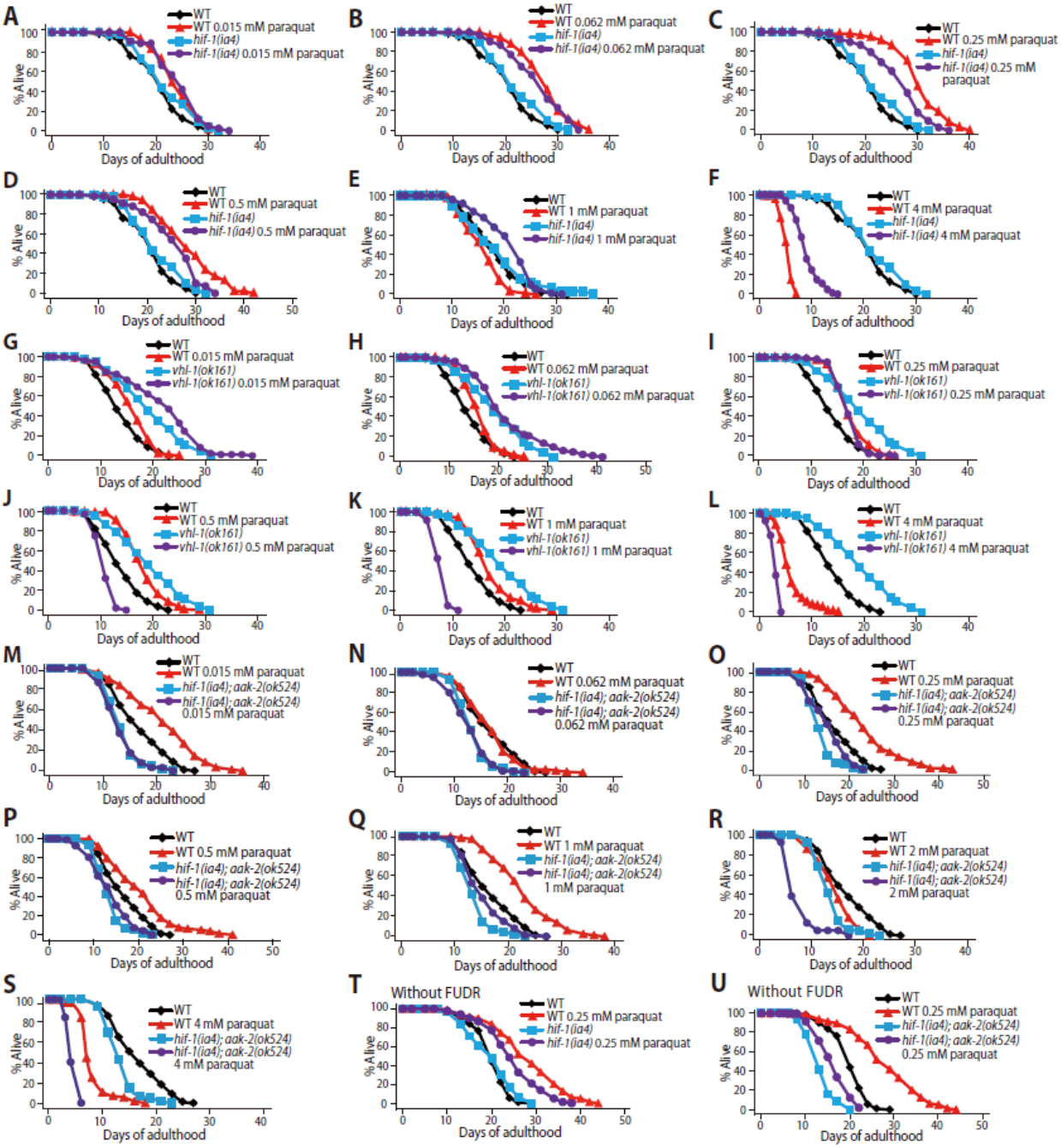

Fig. S4. The lifespan of *hif-1*, *vhl-1*, and *hif-1; aak-2* mutants treated with various concentrations of paraquat. (**A**) Representative lifespan curves of wild-type and *hif-1(ia4)*, wild-type and *vhl-1(ok161)*, and wild-type and *hif-1(ia4); aak-2(ok524)* animals treated with

0.015 mM (**A, G** and **M**), 0.062 mM (**B, H** and **N**), 0.25 mM (**C, I** and **O**), 0.5 mM (**D, J** and **P**), 1 mM (**E, K** and **Q**), 2 mM (**R**), and 4 mM (**F**, **L** and **S**) paraquat during adulthood as indicated. (**T- U**) Lifespan of *hif-1* and *hif-1; aak-2* mutants treated with paraquat (0.25 mM) was measured without FUDR. See **Table S3** for statistical analysis and additional repeats.

Fig. S5

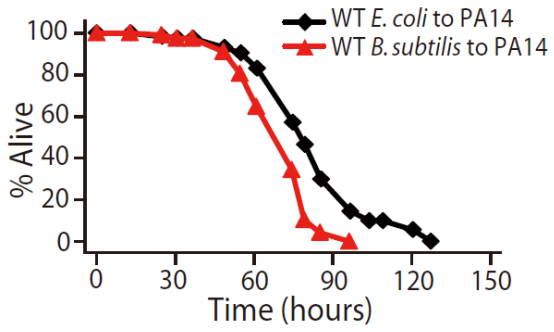

Fig. S5. Preconditioning of non-pathogenic *Bacillus subtilis* decreases the survival of animals on *Pseudomonas aeruginosa*. Wild-type animals transferred from *B. subtilis* to *P. aeruginosa* (PA14) at L4 to young adult stage displayed reduced resistance against PA14 compared to those transferred from OP50 *E. coli.* See **Table S5** for statistical analysis and additional repeats.

Fig. S6

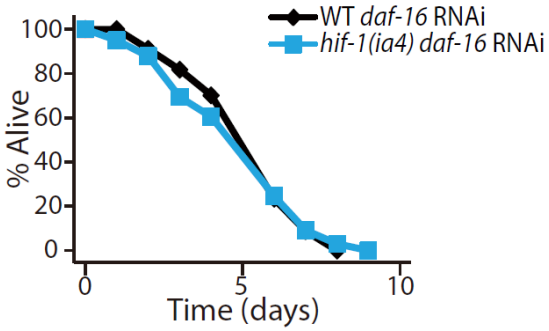

Fig. S6. Survival analysis of wild type and *hif-1* mutant animals treated with *daf-16* RNAi on pathogenic *E. coli*. RNAi targeting *daf-16* abolished the enhanced resistance against pathogenic *E. coli* in *hif-1* mutants at 25˚C. This is consistent with the previous finding that *hif-1* mutants show a temperature-dependent longevity phenotype that requires DAF-16 (14), a well-known transcription factor that mediates longevity and pathogen resistance. See **Table S6** for statistical analysis and additional repeats.

Supporting Tables

Table S1. The effect of 0.25 mM paraquat treatment on the lifespan of *C. elegans*.

Strain/treatment	Mean lifespan ±SEM (days)	75th percentile	% change$^{\Delta}$	Number of animals that died/total	p-value vs. control	Figure in text
WT/control	18.5±0.4	21		169/198		
	18.7±0.5	23		118/151		Fig. S1A
	18.2±0.4	23		125/162		
	18.1±0.5	23		121/150		
	18.3±0.4	22		140/162		Fig. 1A
WT/paraquat	24.7±0.5	30	+34%	169/180	<0.0001	
	28.0±0.6	33	+50%	133/148	<0.0001	Fig. S1A
	21.3±0.5	26	+17%	97/162	<0.0001	
	21.2±0.5	25	+17%	119/150	0.0004	
	26.2±0.4	30	+43%	129/162	<0.0001	Fig. 1A
aak-2(ok524) /control	14.3±0.2	17	-23%	130/180	<0.0001	
	15.7±0.3	19	-16%	125/180	<0.0001	
	13.2±0.3	15	-27%	114/162	<0.0001	
	13.5±0.3	18	-25%	128/150	<0.0001	
	14.2±0.3	17	-22%	145/162	<0.0001	Fig. 1A
aak-2(ok524) /paraquat	15.7±0.2	19	+10% (-15%$^{\text{WT ctrl}}$)	165/182	<0.0001 (<0.0001$^{\text{WT par}}$)	
	17.0±0.3	19	+8% (-9%$^{\text{WT ctrl}}$)	124/150	0.0007 (<0.0001$^{\text{WT par}}$)	
	11.8±0.2	14	-11% (-35%$^{\text{WT ctrl}}$)	121/162	0.0001 (<0.0001$^{\text{WT par)}}$	
	11.9±0.3	15	-12% (-34%$^{\text{WT ctrl}}$)	124/150	0.0015 (<0.0001$^{\text{WT par}}$)	

	13.3±0.4	17	-6% (-27%$^{WT\ ctrl}$)	131/162	0.0997 (<0.0001$^{WT\ par}$)	Fig. 1A
sir-2.1(ok434) /control	18.3±0.4	21	-1%	119/162	0.2213	
	16.8±0.3	19	-10%	147/180	0.0001	Fig. S1A
sir-2.1(ok434) /paraquat	22.2±0.4	26	+21% (+20%$^{WT\ ctrl}$)	162/185	<0.0001 (<0.0001$^{WT\ par}$)	
	23.0±0.4	27	+37% (+23%$^{WT\ ctrl}$)	141/153	<0.0001 (<0.0001$^{WT\ par}$)	Fig. S1A
WT/control without FUDR^	17.1±0.4	21		147/244		
$	14.2±0.4	17		59/125		
*	20.2±0.4	24		108/175		Fig. 1B, S4T, S4U
WT/paraquat without FUDR^	21.1±0.4	25	+23%	118/180	<0.0001	
$	23.1±0.6	27	+63%	105/180	<0.0001	
*	28.1±0.7	34	+39%	96/160	<0.0001	Fig. 1B, S4T, S4U
aak-2(ok524) /control without FUDR	14.0±0.4	16	-18%	83/150	<0.0001	
	12.7±0.4	15	-10%	72/150	0.0105	
	15.5±0.4	20	-23%	90/315	<0.0001	Fig. 1B
aak-2(ok524) /paraquat without FUDR	13.9±0.3	16	-1% (-19%$^{WT\ ctrl}$)	119/170	0.3417 (<0.0001$^{WT\ par}$)	
	13.2±0.2	15	+4% (-7%$^{WT\ ctrl}$)	113/165	0.675 (<0.0001$^{WT\ par}$)	
	15.0±0.4	17	-3% (-26%$^{WT\ ctrl}$)	96/207	0.2462 (<0.0001$^{WT\ par}$)	Fig. 1B
WT/control	19.9±0.5	25		121/147		Fig. 1C
	16.4±0.5	20		126/150		
WT/paraquat	26.0±0.5	31	+31%	130/153	<0.0001	Fig. 1C

	30.6±0.6	36	+87%	137/150	<0.0001	
aak-2(rr48) /control	15.5±0.3	17	-22%	100/150	<0.0001	Fig. 1C
	13.3±0.3	17	-19%	115/150	<0.0001	
aak-2(rr48) /paraquat	15.0±0.3	17	-3% (-25%$^{WT\ ctrl}$)	118/148	0.5173 (<0.0001$^{WT\ par}$)	Fig. 1C
	15.7±0.5	20	+18% (-4%$^{WT\ ctrl}$)	108/150	<0.0001 (<0.0001$^{WT\ par}$)	
WT/control	20.1±0.6	25		89/100		Fig. 1D,1E
	18.5±0.5	23		95/100		
WT/paraquat	27.4±0.9	33	+36%	78/100	<0.0001	Fig. 1D,1E
	22.2±0.6	27	+20%	91/100	<0.0001	
aakb-2(rr88) /control	16.8±0.5	22	-16%	74/100	<0.0001	Fig. 1D
	16.2±0.5	19	-12%	70/75	0.0006	
aakb-2(rr88) /paraquat	15.2±0.8	21	-10% (-24%$^{WT\ ctrl}$)	57/120	0.1603 (<0.0001$^{WT\ par}$)	Fig. 1D
	15.5±0.5	19	-4% (-16%$^{WT\ ctrl}$)	93/120	0.7463 (<0.0001$^{WT\ par}$)	
par-4(tm2986) /control	18.3±0.8	23	-9%	53/100	0.0136	Fig. 1E
	17.3±0.6	21	-6%	77/100	0.2001	
par-4(tm2986) /paraquat	21.4±0.7	25	+17% (+6%$^{WT\ ctrl}$)	77/102	0.0053 (<0.0001$^{WT\ par}$)	Fig. 1E
	19.4±0.5	23	+12% (+5%$^{WT\ ctrl}$)	78/100	0.0301 (<0.0001$^{WT\ par}$)	
Control transgenic (IJ599) /control	19.5±0.6	23		108/150		Fig. 1I, IJ
	18.9±0.5	24		134/150		
Control transgenic (IJ599) /paraquat	26.3±0.7	31	+35%	92/150	<0.0001	Fig. 1I, IJ
	23.6±0.6	29	+25%	117/155	<0.0001	
CA-aak-2::gfp (IJ600) /control	25.3±0.6	30	+30%	106/120	<0.0001	Fig. 1I, IJ

	25.4±0.4	28	+34%	109/120	<0.0001	
CA-aak-2::gfp (IJ600) /paraquat	27.8±0.5	33	+10% (+43%$^{\text{Ctrl Tg ctrl}}$)	131/150	0.0008 (0.1852$^{\text{Ctrl Tg par}}$)	Fig. 1I, IJ
	26.8±0.4	31	+6% (+42%$^{\text{Ctrl Tg ctrl}}$)	140/155	0.0004 (0.0004$^{\text{Ctrl Tg par}}$)	
Control transgenic (WMB59$^{\#}$) /control	19.8±0.7	24		49/60		
	20.1±0.5	23		74/90		
Control transgenic (WMB59$^{\#}$) /paraquat	22.4±0.7	26	+13%	74/90	0.0008	
	23.5±0.7	29	+17%	77/90	0.0002	
CA-aak-2::gfp (WMB60$^{\#}$) /control	23.3±0.4	26	+18%	55/60	0.0003 (0.3602$^{\text{Ctrl Tg par}}$)	
	23.4±0.4	26	+16%	79/90	0.0017 (0.0497$^{\text{Ctrl Tg par}}$)	
CA-aak-2::gfp (WMB60$^{\#}$) /paraquat	22.8±0.6	26	-2% (+15%$^{\text{Ctrl Tg ctrl}}$)	83/90	0.3009 (0.8885$^{\text{Ctrl Tg par}}$)	
	22.7±0.5	25	-3% (+13%$^{\text{Ctrl Tg ctrl}}$)	71/90	0.4750 (0.0527$^{\text{Ctrl Tg par}}$)	
WT/control	20.4±0.4	24		130/162		Fig. S1B
	20.7±0.5	25		124/150		
WT/paraquat	24.4±0.5	31	+20%	114/162	<0.0001	Fig. S1B
	27.6±0.5	31	+33%	101/145	<0.0001	
hsf-1(sy441) /control	16.3±0.3	20	-20%	129/162	<0.0001	Fig. S1B
	16.6±0.3	20	-20%	115/150	<0.0001	
hsf-1(sy441) /paraquat	18.9±0.4	25	+16% (-7%$^{\text{WT ctrl}}$)	112/142	<0.0001 (<0.0001$^{\text{WT par}}$)	Fig. S1B
	20.1±0.3	23	+21% (-3%$^{\text{WT ctrl}}$)	115/150	<0.0001 (<0.0001$^{\text{WT par}}$)	
WT/control	14.3±0.3	17		104/121		

	15.1±0.4	19		106/120		Fig. S1C
WT/paraquat	17.8±0.3	21	+24%	98/120	<0.0001	
	21.0±0.4	23	+39%	101/120	<0.0001	Fig. S1C
daf-12 (rh61rh411) /control	12.6±0.4	15	-12%	104/120	0.0020	
	12.6±0.4	13	-17%	110/120	<0.0001	Fig. S1C
daf-12 (rh61rh411) /paraquat	21.6±0.6	26	+71% ($+51\%^{WT\ ctrl}$)	102/125	<0.0001 ($<0.0001^{WT\ par}$)	
	21.3±0.4	23	+69% ($+41\%^{WT\ ctrl}$)	102/120	<0.0001 ($0.3896^{WT\ par}$)	Fig. S1C
WT/control	19.2±0.5	22		78/100		Fig. S1D
	19.5±0.5	22		83/100		
WT/paraquat	28.2±0.7	33	+47%	88/100	<0.0001	Fig. S1D
	25.4±0.7	31	+30%	85/100	<0.0001	
skn-1(zu67) /control	13.0±0.5	16	-32%	66/71	<0.0001	Fig. S1D
	13.1±0.4	16	-33%	62/100	<0.0001	
skn-1(zu67) /paraquat	19.8±0.8	25	+52% ($+3\%^{WT\ ctrl}$)	58/60	<0.0001 ($<0.0001^{WT\ par}$)	Fig. S1D
	26.3±1.1	34	+101% ($+35\%^{WT\ ctrl}$)	59/62	<0.0001 ($0.1420^{WT\ par}$)	
WT/control	18.1±0.5	22		135/150		Fig. S1E
	17.0±0.4	21		134/150		
WT/paraquat	26.8±0.7	33	+48%	113/150	<0.0001	Fig. S1E
	28.5±0.6	33	+68%	111/150	<0.0001	
haf-1(ok705) /control	17.7±0.5	22	-2%	129/150	0.6852	Fig. S1E
	18.7±0.5	21	+10%	116/150	0.0085	
haf-1(ok705) /paraquat	26.4±0.7	31	+49% ($+46\%^{WT\ ctrl}$)	117/150	<0.0001 ($0.8613^{WT\ par}$)	Fig. S1E
	28.0±0.7	33	+50% ($+64\%^{WT\ ctrl}$)	80/150	<0.0001 ($0.5128^{WT\ par}$)	

Within this table and other tables, the survival data sets shaded in the same colors (white or grey) were done in parallel within the solid line and statistical analysis was done within the data set. p-values were calculated using the log-rank (Mantel-Cox) method.

$^{\Delta}$: throughout **Tables S1-S6**, % change in survival was calculated against the same control data. Increased (+) or decreased (-) mean survival was indicated.

$\%^{\text{WT ctrl}}$ and $\%^{\text{Ctrl Tg ctrl}}$: the % change in mean lifespan compared to the control condition of wild-type or control-transgenic animals, respectively. The average of these percent values was used for the "% change in lifespan" in **Fig. 1F** or **Fig. 1J**.

p-values for single mutants were calculated against wild-type animals and for paraquat-treated mutants against control mutants. p-values in the parentheses ($^{\text{WT par}}$ and $^{\text{Ctrl Tg par}}$) are the p-values against wild-type and control transgenic animals treated with 0.25 mM paraquat, respectively.

$^{\wedge}$, $^{\$}$, *: the lifespan data marked with these are also used in **Table S3**.

$^{\#}$: We noticed that 0.25 mM paraquat treatment had only a small life-extending effect on the control transgenic animals (WBM59). We therefore performed four additional outcrosses for both control (co-injection marker only) and the *aak-2* transgenic animals. The newly outcrossed control animals (IJ599) significantly lived long upon 0.25 mM paraquat treatment (**Figures 1I and 1J**).

Table S2. The effect of various doses of paraquat on the lifespan of *aak-2* mutants and *aak-2*-overexpressing transgenic animals.

Strain/treatment	Mean lifespan ±SEM (days)	75th percentile	% change[Δ]	Number of animals that died/total	p-value vs. control	Figure in text
WT/control[@]	14.1±0.4	17		82/90		
[@]	16.4±0.4	19		106/120		Fig. S3A-S3F
WT/0.015 mM paraquat[@]	16.1±0.4	19	+14%	102/120	0.0019	
[@]	18.6±0.4	21	+13%	97/120	0.0002	Fig. S3A
WT/0.062 mM paraquat[@]	16.1±0.4	19	+14%	54/60	0.0152	
[@]	20.0±0.4	23	+22%	103/119	<0.0001	Fig. S3B
WT/0.25 mM paraquat[@]	17.7±0.3	19	+26%	94/120	<0.0001	
[@]	23.0±0.4	25	+40%	107/120	<0.0001	Fig. S3C
WT/0.5 mM paraquat[@]	18.4±0.4	21	+30%	112/120	<0.0001	
[@]	25.8±0.5	30	+57%	92/120	<0.0001	Fig. S3D
WT/1 mM paraquat[@]	17.2±0.4	19	+22%	109/120	<0.0001	
[@]	22.2±0.5	25	+35%	100/120	<0.0001	Fig. S3E
WT/4 mM paraquat[@]	6.0±0.3	7	-57%	81/90	<0.0001	
[@]	7.4±0.3	9	-55%	70/120	<0.0001	Fig. 3B, S3F
aak-2(ok524) /control	11.7±0.4	15	-17%	48/90	0.0002	

	13.4±0.3	15	-18%	81/120	<0.0001	Fig. S3A-S3F
aak-2(ok524) /0.015 mM paraquat	12.4±0.5	15	+6% (-12%$^{\text{WT ctrl}}$)	63/120	0.2002 (<0.0001 $^{\text{WT 0.015 mM par}}$)	
	16.2±0.5	19	+21% (-1%$^{\text{WT ctrl}}$)	48/90	<0.0001 (0.0001 $^{\text{WT 0.015 mM par}}$)	Fig. S3A
aak-2(ok524) /0.062 mM paraquat	13.9±0.4	17	+19% (-1%$^{\text{WT ctrl}}$)	83/120	0.0001 (0.0015 $^{\text{WT 0.062 mM par}}$)	
	17.2±0.4	19	+28% (+5%$^{\text{WT ctrl}}$)	69/120	<0.0001 (<0.0001 $^{\text{WT 0.062 mM par}}$)	Fig. S3B
aak-2(ok524) /0.25 mM paraquat	12.0±0.5	15	+3% (-15%$^{\text{WT ctrl}}$)	71/90	0.4193 (<0.0001 $^{\text{WT 0.25 mM par}}$)	
	14.1±0.5	17	+5% (-14%$^{\text{WT ctrl}}$)	90/120	0.0647 (<0.0001 $^{\text{WT 0.25 mM par}}$)	Fig. S3C
aak-2(ok524) /0.5 mM paraquat	9.4±0.3	13	-20% (-33%$^{\text{WT ctrl}}$)	108/120	0.0015 (<0.0001 $^{\text{WT 0.5 mM par}}$)	
	12.2±0.4	15	-9% (-26%$^{\text{WT ctrl}}$)	107/120	0.2043 (<0.0001 $^{\text{WT 0.5 mM par}}$)	Fig. S3D
aak-2(ok524) /1 mM paraquat	8.7±0.4	11	-26% (-38%$^{\text{WT ctrl}}$)	86/120	<0.0001 (<0.0001 $^{\text{WT 1 mM par}}$)	
	10.5±0.5	13	-22% (-36%$^{\text{WT ctrl}}$)	75/104	<0.0001 (<0.0001 $^{\text{WT 1 mM par}}$)	Fig. S3E
aak-2(ok524) /4 mM paraquat	2.2±0.1	3	-81% (-84%$^{\text{WT ctrl}}$)	48/90	<0.0001 (<0.0001 $^{\text{WT 4 mM par}}$)	
	2.1±0.1	3	-84% (-87%$^{\text{WT ctrl}}$)	47/90	<0.0001 (<0.0001 $^{\text{WT 4 mM par}}$)	Fig. 3B, S3F
Control transgenic (IJ599)/4 mM paraquat	9.2±0.3	12		95/100		Fig. 3C
	13.5±0.5	18		89/100		
CA-aak-2::gfp	10.9±0.4	14	+19%	95/100	0.0001	Fig. 3C

(IJ600)/4 mM paraquat						
	15.1±0.6	19	+12%	87/100	0.003	
Control transgenic (WBM59[#])/4 mM paraquat	3.9±0.1	5		53/60		
	4.5±0.1	7		51/60		
CA-aak-2::gfp (WBM60[#])/4 mM paraquat	5.7±0.2	7	+46%	57/60	<0.0001	
	6.9±0.2	9	+53%	59/60	<0.0001	

Within this table, paraquat treatment was started from L4 stage throughout adulthood.

[Δ]: throughout **Tables S2-S3**, % changes in lifespan were calculated against the same control data. Increased (+) or decreased (-) mean lifespan was indicated.

$\%^{\text{WT ctrl}}$: the % change was calculated against the lifespan compared to wild-type control. The average of these percentages was used for the "% change in lifespan" in **Figure 3A**.

p-values for mutants were calculated against wild type, and for mutants or transgenic animals treated with paraquat against the mutants under control condition and control transgenic (Tg) animals, respectively. p-values in the parentheses were calculated against wild type treated with the indicated concentration of paraquat (par).

[@]: the lifespan data marked with this are also used in **Table S3**.

[#]: We noticed that the survival time of control transgenic animals (WBM59) were substantially short upon 4 mM paraquat treatment. We performed four additional outcrosses for both control (co-injection marker only) (IJ599) and the *aak-2* transgenic animals (IJ600) for **Figure 3C**.

Table S3. The effect of various doses of paraquat treatment on the lifespan of *hif-1*, *vhl-1*, and *hif-1; aak-2* mutants.

Strain/treatment	Mean lifespan ±SEM (days)	75th percentile	% change$^{\Delta}$	Number of animals that died/total	p-value vs. control	Figure in text
WT/control	21.4±0.6	24		72/83		
	20.6±0.6	23		63/75		Fig. S4A-S4F
	22.7±0.6	26		52/90		
	18.2±0.5	21		90/100		
	16.7±0.5	18		85/98		
WT/0.015 mM paraquat	20.4±0.5	24	-5%	71/85	0.3243	
	24.3±0.5	28	+18%	59/75	0.0002	Fig. S4A
	23.6±0.6	28	+4%	55/90	0.1621	
	22.0±0.8	26	+21%	68/100	<0.0001	
	21.2±0.6	26	+27%	75/100	<0.0001	
WT/0.062 mM paraquat	23.3±0.6	26	+9%	77/86	0.0137	
	27.7±0.7	30	+34%	44/73	<0.0001	Fig. S4B
	25.4±0.7	30	+12%	60/82	0.0006	
	23.4±0.7	26	+29%	73/100	<0.0001	
	22.2±0.6	26	+33%	75/100	<0.0001	
WT/0.25 mM paraquat	26.8±0.7	32	+25%	63/87	<0.0001	
	30.6±0.6	34	+49%	58/75	<0.0001	Fig. S4C
	27.0±0.7	30	+19%	72/90	<0.0001	
	24.4±1.0	30	+34%	66/100	<0.0001	
	24.8±0.8	28	+49%	67/100	<0.0001	
WT/0.5 mM paraquat	23.9±0.8	28	+12%	71/87	0.0009	

	28.7±0.8	32	+39%	50/75	<0.0001	Fig. S4D
	22.1±0.7	28	-3%	76/90	0.4704	
	19.0±0.6	24	+4%	90/100	0.2491	
	21.2±0.6	26	+27%	74/100	<0.0001	
WT/1 mM paraquat	19.2±0.6	22	-10%	78/80	0.0223	
	22.3±0.7	25	+8%	64/75	0.1055	Fig. S4E
	13.4±0.3	16	-41%	64/90	<0.0001	
	16.0±0.4	19	-12%	93/100	0.0003	
	17.0±0.4	21	+2%	91/100	0.9697	
WT/4 mM paraquat	3.9±0.1	5	-82%	58/90	<0.0001	
	5.4±0.1	7	-74%	68/90	<0.0001	Fig. S4F
	6.5±0.2	8	-71%	73/90	<0.0001	
	6.9±0.1	8	-62%	80/90	<0.0001	
	7.7±0.2	9	-54%	103/135	<0.0001	
hif-1(ia4)/control	20.5±0.8	24	-4%	45/90	0.5797	
	22.1±0.9	28	+7%	33/75	0.1683	Fig. S4A-S4F
	19.7±0.8	24	-13%	41/90	0.0107	
	18.7±0.7	23	+3%	87/100	0.3922	
	19.3±0.6	25	+16%	78/100	0.0007	
hif-1(ia4) /0.015 mM paraquat	23.4±0.7	26	+14% (+9%$^{\text{WT ctrl}}$)	50/83	0.0215 (0.0002 $^{\text{WT 0.015 mM par}}$)	
	24.5±0.7	28	+11% (+19%$^{\text{WT ctrl}}$)	41/75	0.0526 (0.4844 $^{\text{WT 0.015 mM par}}$)	Fig. S4A
	21.9±0.8	26	+11% (-4%$^{\text{WT ctrl}}$)	53/90	0.0272 (0.2305 $^{\text{WT 0.015 mM par}}$)	
	22.3±1.0	29	+19% (23%$^{\text{WT ctrl}}$)	60/100	0.0048 (0.5159 $^{\text{WT 0.015 mM par}}$)	

	20.4±0.6	25	+6% (+22%$^{WT\ ctrl}$)	58/85	0.3043 (0.1409 $^{WT\ 0.015\ mM\ par}$)	
hif-1(ia4) /0.062 mM paraquat	22.2±0.7	26	+8% (+4%$^{WT\ ctrl}$)	63/71	0.1556 (0.5092 $^{WT\ 0.062\ mM\ par}$)	
	26.3±0.7	30	+19% (+28%$^{WT\ ctrl}$)	58/75	0.0002 (0.2830 $^{WT\ 0.062\ mM\ par}$)	Fig. S4B
	24.5±0.7	28	+24% (+8%$^{WT\ ctrl}$)	51/90	<0.0001 (0.2097 $^{WT\ 0.062\ mM\ par}$)	
	21.5±0.6	25	+15% (+18%$^{WT\ ctrl}$)	80/100	0.0203 (0.0073 $^{WT\ 0.062\ mM\ par}$)	
	20.8±0.4	22	+8% (+25%$^{WT\ ctrl}$)	96/107	0.2024 (0.0039 $^{WT\ 0.062\ mM\ par}$)	
hif-1(ia4) /0.25 mM paraquat	25.2±0.8	30	+23% (+18%$^{WT\ ctrl}$)	64/73	0.0001 (0.2425 $^{WT\ 0.25\ mM\ par}$)	
	26.5±0.7	30	+20% (+29%$^{WT\ ctrl}$)	65/75	0.0001 (<0.0001 $^{WT\ 0.25\ mM\ par}$)	Fig. S4C
	26.3±0.7	30	+34% (+16%$^{WT\ ctrl}$)	79/90	<0.0001 (0.5805 $^{WT\ 0.25\ mM\ par}$)	
	22.0±0.8	26	+18% (+21%$^{WT\ ctrl}$)	76/100	0.0060 (0.0368 $^{WT\ 0.25\ mM\ par}$)	
	22.7±0.6	27	+18% (+36%$^{WT\ ctrl}$)	65/98	0.0003 (0.0086 $^{WT\ 0.25\ mM\ par}$)	
hif-1(ia4) /0.5 mM paraquat	22.9±0.7	26	+12% (+7%$^{WT\ ctrl}$)	75/87	0.0313 (0.1590 $^{WT\ 0.5\ mM\ par}$)	
	25.6±0.7	30	+16% (+24%$^{WT\ ctrl}$)	68/75	0.0008 (0.0028 $^{WT\ 0.5\ mM\ par}$)	Fig. S4D
	22.2±0.7	26	+13% (-2%$^{WT\ ctrl}$)	76/90	0.0124 (0.9014 $^{WT\ 0.5\ mM\ par}$)	
	21.2±0.6	25	+13% (+16%$^{WT\ ctrl}$)	92/100	0.0353 (0.0170 $^{WT\ 0.5\ mM\ par}$)	

	21.9±0.5	25	+13% (+31%$^{WT\ ctrl}$)	91/100	0.0062 (0.4687 $^{WT\ 0.5\ mM\ par}$)	
hif-1(ia4) /1 mM paraquat	18.8±0.5	22	-8% (-12%$^{WT\ ctrl}$)	65/75	0.0205 (0.6271 $^{WT\ 1\ mM\ par}$)	
	22.5±0.4	25	+2% (+9%$^{WT\ ctrl}$)	63/75	0.9482 (0.8792 $^{WT\ 1\ mM\ par}$)	Fig. S4E
	16.5±0.5	18	-16% (-27%$^{WT\ ctrl}$)	72/90	<0.0001 (<0.0001 $^{WT\ 1\ mM\ par}$)	
	21.1±0.5	25	+13% (+16%$^{WT\ ctrl}$)	93/100	0.0390 (<0.0001 $^{WT\ 1\ mM\ par}$)	
	20.0±0.5	22	+4% (+20%$^{WT\ ctrl}$)	86/100	0.6769 (<0.0001 $^{WT\ 1\ mM\ par}$)	
hif-1(ia4) /4 mM paraquat	7.9±0.4	10	-61% (-63%$^{WT\ ctrl}$)	86/90	<0.0001 (<0.0001 $^{WT\ 4\ mM\ par}$)	
	9.1±0.3	10	-59% (-56%$^{WT\ ctrl}$)	82/90	<0.0001 (<0.0001 $^{WT\ 4\ mM\ par}$)	Fig. S4F
	11.2±0.3	13	-43% (-51%$^{WT\ ctrl}$)	79/82	<0.0001 (<0.0001 $^{WT\ 4\ mM\ par}$)	
	9.9±0.3	11	-47% (-45%$^{WT\ ctrl}$)	85/90	<0.0001 (<0.0001 $^{WT\ 4\ mM\ par}$)	
	9.6±0.2	11	-50% (-43%$^{WT\ ctrl}$)	91/105	<0.0001 (<0.0001 $^{WT\ 4\ mM\ par}$)	
WT/control[@]	14.1±0.4	17		82/90		Fig. S4G-S4L
[@]	16.4±0.4	19		106/120		
WT/0.015 mM paraquat[@]	16.1±0.4	19	+14%	102/120	0.0019	Fig. S4G
[@]	18.6±0.4	21	+13%	97/120	0.0002	
WT/0.062 mM paraquat[@]	16.1±0.4	19	+14%	54/60	0.0152	Fig. S4H

[@]	20.0±0.4	23	+22%	103/119	<0.0001	
WT/0.25 mM paraquat[@]	17.7±0.3	19	+26%	94/120	<0.0001	Fig. S4I
[@]	23.0±0.4	25	+40%	107/120	<0.0001	
WT/0.5 mM paraquat[@]	18.4±0.4	21	+30%	112/120	<0.0001	Fig. S4J
[@]	25.8±0.5	30	+57%	92/120	<0.0001	
WT/1 mM paraquat[@]	17.2±0.4	19	+22%	109/120	<0.0001	Fig. S4K
[@]	22.2±0.5	25	+35%	100/120	<0.0001	
WT/4 mM paraquat[@]	6.0±0.3	7	-57%	81/90	<0.0001	Fig. S4L
[@]	7.4±0.3	9	-55%	70/120	<0.0001	
vhl-1(ok161) /control	19.4±0.7	25	+38%	74/90	<0.0001	Fig. S4G-S4L
	22.2±0.6	27	+35%	92/120	<0.0001	
vhl-1(ok161) /0.015 mM paraquat	21.8±0.8	26	+12% (+55%$^{\text{WT ctrl}}$)	86/120	0.0088 (<0.0001 $_{\text{WT 0.015 mM par}}$)	Fig. S4G
	25.8±0.7	30	+16% (+57%$^{\text{WT ctrl}}$)	78/90	0.0001 (<0.0001 $_{\text{WT 0.015 mM par}}$)	
vhl-1(ok161) /0.062 mM paraquat	21.6±0.8	25	+11% (+53%$^{\text{WT ctrl}}$)	82/120	0.0362 (<0.0001 $_{\text{WT 0.062 mM par}}$)	Fig. S4H
	24.5±0.6	30	+10% (+49%$^{\text{WT ctrl}}$)	112/120	0.0035 (<0.0001 $_{\text{WT 0.062 mM par}}$)	
vhl-1(ok161) /0.25 mM paraquat	17.4±0.3	19	-10% (+23%$^{\text{WT ctrl}}$)	89/120	0.0001 (0.3833 $_{\text{WT 0.25 mM par}}$)	Fig. S4I
	21.7±0.4	25	-2% (+32%$^{\text{WT ctrl}}$)	105/120	0.0783 (0.0325 $_{\text{WT 0.25 mM par}}$)	
vhl-1(ok161) /0.5 mM paraquat	11.1±0.2	13	-43% (-21%$^{\text{WT ctrl}}$)	102/120	<0.0001 (<0.0001 $_{\text{WT 0.5 mM par}}$)	Fig. S4J
	15.3±0.3	17	-31%	109/120	<0.0001	

			(-7%$^{\text{WT ctrl}}$)		(<0.0001 $^{\text{WT 0.5 mM par}}$)	
vhl-1(ok161) /1 mM paraquat	8.0±0.1	11	-59% (-43%$^{\text{WT ctrl}}$)	110/120	<0.0001 (<0.0001 $^{\text{WT 1 mM par}}$)	Fig. S4K
	11.7±0.3	15	-47% (-29%$^{\text{WT ctrl}}$)	110/120	<0.0001 (<0.0001 $^{\text{WT 1mM par}}$)	
vhl-1(ok161) /4 mM paraquat	3.1±0.1	4	-84% (-78%$^{\text{WT ctrl}}$)	60/90	<0.0001 (<0.0001 $^{\text{WT 4mM par}}$)	Fig. S4L
	4.1±0.2	7	-82% (-75%$^{\text{WT ctrl}}$)	73/90	<0.0001 (<0.0001 $^{\text{WT 4mM par}}$)	
WT/control	18.0±0.5	21		85/100		
	16.7±0.5	21		79/100		Fig. S5M-S5S
WT /0.015 mM paraquat	23.9±0.6	29	+33%	81/100	<0.0001	
	21.1±0.7	27	+26%	83/100	<0.0001	Fig. S5M
WT /0.062 mM paraquat	23.9±0.6	29	+33%	84/100	<0.0001	
	22.9±0.7	27	+37%	79/100	<0.0001	Fig. S5N
WT/0.25 mM paraquat	25.8±0.8	31	+43%	82/100	<0.0001	
	23.3±0.8	27	+40%	84/100	<0.0001	Fig. S5O
WT/0.5 mM paraquat	23.9±0.8	27	+33%	86/100	<0.0001	
	20.6±0.8	25	+23%	79/100	<0.0001	Fig. S5P
WT/1 mM paraquat	19.3±0.5	23	+7%	94/100	0.0996	
	16.9±0.5	19	+1%	90/100	0.9850	Fig. S5Q
WT/2 mM paraquat	16.0±0.5	19	-11%	93/100	0.0027	
	14.6±0.4	17	-13%	91/100	0.0002	Fig. S5R
WT/4 mM	10.5±0.5	14	-42%	47/90	<0.0001	

paraquat						
	8.2±0.4	10	-51%	58/90	<0.0001	Fig. S5S
hif-1(ia4); aak-2(ok524)/control	15.0±0.6	17	-17%	42/108	<0.0001	
	13.6±0.4	15	-19%	63/117	<0.0001	Fig. S5M-S5S
hif-1(ia4); aak-2(ok524) /0.015 mM paraquat	16.2±0.6	19	+8% (-10%$^{\text{WT ctrl}}$)	48/108	0.1232 (<0.0001 $^{\text{WT 0.015 mM par}}$)	
	13.3±0.4	15	-2% (-20%$^{\text{WT ctrl}}$)	66/120	0.6512 (<0.0001 $^{\text{WT 0.015 mM par}}$)	Fig. S5M
hif-1(ia4); aak-2(ok524) /0.062 mM paraquat	19.5±0.6	23	+30% (+8%$^{\text{WT ctrl}}$)	49/108	0.0001 (<0.0001 $^{\text{WT 0.062 mM par}}$)	
	15.4±0.5	17	+13% (-8%$^{\text{WT ctrl}}$)	73/120	0.0033 (<0.0001 $^{\text{WT 0.062 mM par}}$)	Fig. S5N
hif-1(ia4); aak-2(ok524) /0.25 mM paraquat	19.5±0.7	23	+30% (+8%$^{\text{WT ctrl}}$)	41/108	0.0001 (<0.0001 $^{\text{WT 0.25 mM par}}$)	
	15.2±0.5	19	+12% (-9%$^{\text{WT ctrl}}$)	75/120	0.0044 (<0.0001 $^{\text{WT 0.25 mM par}}$)	Fig. S5O
hif-1(ia4); aak-2(ok524)/0.5 mM paraquat	17.9±0.6	21	+19% (-1%$^{\text{WT ctrl}}$)	58/108	0.0009 (<0.0001 $^{\text{WT 0.5 mM par}}$)	
	13.8±0.5	17	+1% (-17%$^{\text{WT ctrl}}$)	72/100	0.3717 (<0.0001 $^{\text{WT 0.5 mM par}}$)	Fig. S5P
hif-1(ia4); aak-2(ok524)/1 mM paraquat	18.7±0.6	23	+25% (+4%$^{\text{WT ctrl}}$)	85/108	0.0001 (0.6715 $^{\text{WT 1 mM par}}$)	
	13.0±0.4	15	-4% (-22%$^{\text{WT ctrl}}$)	64/84	0.5571 (<0.0001 $^{\text{WT 1 mM par}}$)	Fig. S5Q
hif-1(ia4); aak-2(ok524)/2 mM paraquat	9.5±0.4	12	-37% (-47%$^{\text{WT ctrl}}$)	81/108	0.0001 (<0.0001 $^{\text{WT 2 mM par}}$)	

	7.6±0.4	11	-44% (-54%$^{WT\ ctrl}$)	48/100	0.0001 (<0.0001 $^{WT\ 2\ mM\ par}$)	Fig. S5R
hif-1(ia4); aak-2(ok524)/4 mM paraquat	5.0±0.2	6	-67% (-72%$^{WT\ ctrl}$)	26/90	0.0001 (<0.0001 $^{WT\ 4\ mM\ par}$)	
	4.6±0.2	6	-66% (-72%$^{WT\ ctrl}$)	25/90	0.0001 (<0.0001 $^{WT\ 4\ mM\ par}$)	Fig. S5S
WT/control, without FUDR$^{\wedge}$	17.1±0.4	21		147/244		
$^{\$}$	14.2±0.4	17		59/125		
*	20.2±0.4	24		108/175		Fig. 1B, S4T, S4U
	18.8±0.4	23		105/175		
WT/0.25 mM paraquat, without FUDR$^{\wedge}$	21.1±0.4	25	+23%	118/180	<0.0001	
$^{\$}$	23.1±0.6	27	+63%	105/180	<0.0001	
*	28.1±0.7	34	+39%	96/160	<0.0001	Fig. 1B, S4T, S4U
	25.7±0.5	31	+37%	115/175	<0.0001	
hif-1(ia4) /control, without FUDR	19.3±0.5	23	+13%	83/125	0.0005	
	17.5±0.5	22	+23%	84/125	<0.0001	
	19.9±0.5	24	-1%	91/140	0.391	Fig. S4T
	21.2±0.5	23	+13%	79/175	0.0001	
hif-1(ia4) /0.25 mM paraquat, without FUDR	19.0±0.6	24	-2% (+11%$^{WT\ ctrl}$)	81/130	0.893 (0.0568$^{WT\ par}$)	
	16.0±0.5	18	-8% (+13%$^{WT\ ctrl}$)	78/150	0.0272 (<0.0001$^{WT\ par}$)	
	24.9±0.6	29	25% (+23%$^{WT\ ctrl}$)	92/140	<0.0001 (0.0002$^{WT\ par}$)	Fig. S4T
	23.6±0.5	27	+11% (+25%$^{WT\ ctrl}$)	98/175	0.0004 (0.0013$^{WT\ par}$)	
hif-1(ia4); aak-2(ok524)	11.2±0.3	14	-35%	80/150	<0.0001	

/control, without FUDR						
	11.1±0.4	13	-22%	53/146	<0.0001	
	13.6±0.3	17	-33%	85/200	<0.0001	Fig. S4U
hif-1(ia4); aak-2(ok524)) /0.25 mM paraquat, without FUDR	14.5±0.4	18	+30% (-15%$^{WT\ ctrl}$)	118/180	<0.0001 (<0.0001$^{WT\ par}$)	
	13.8±0.3	18	+24% (-3%$^{WT\ ctrl}$)	118/162	<0.0001 (<0.0001$^{WT\ par}$)	
	16.5±0.3	20	+21% (-18%$^{WT\ ctrl}$)	146/244	<0.0001 (<0.0001$^{WT\ par}$)	Fig. S4U

Within this table, paraquat treatment was started from L4 stage throughout adulthood. For lifespan measurements without FUDR treatment, paraquat treatment was started from egg hatching.

$^{\Delta}$: % changes in lifespan were calculated against the same control data. Increased (+) or decreased (-) mean lifespan was indicated.

%$^{WT\ ctrl}$: the % change in lifespan compared to wild-type control. The average of these percentage values was used for the "% change in lifespan" in **Figures 4A**, **4E**, or **4J**

p-values were calculated for mutants against wild type and for paraquat-treated mutants against the corresponding mutants under control condition. p-values in the parentheses were calculated against wild type treated with the indicated concentration of paraquat (par)

$^{\wedge}$, $^{\$}$, *: the lifespan data marked with these are also used in **Table S1**.

$^{@}$: The lifespan data marked with these are also used in **Table S2**.

Table S4. Lifespan analysis of *isp-1* and *isp-1; hif-1* mutants treated with RNAi targeting iron-homeostasis regulatory genes.

Strain/treatment	Mean lifespan ±SEM (days)	75th percentile	% change$^{\Delta}$	Number of animals that died/total	p-value vs. control	Figure in text
WT /control RNAi	22.7±0.4	25		131/150		Fig. 5C, 5E, 5G, 5H
	21.9±0.4	27		137/150		
	18.4±0.4	22		127/150		
WT /*smf-3* RNAi	23.6±0.4	28	+4%	99/145	0.0818	Fig. 5G
	21.3±0.4	24	-2%	132/150	0.2967	
	19.0±0.4	22	+3%	133/150	0.6412	
WT /*ftn-1*/*ftn-2* RNAi	24.8±0.6	29	+10%	124/150	<0.0001	Fig. 5H
	24.3±0.5	28	+11%	127/150	<0.0001	
	19.4±0.5	22	+6%	104/121	0.1249	
hif-1(ia4) /control RNAi	23.4±0.5	28	+3%	93/121	0.0833	Fig. 5G, 5H
	22.7±0.5	25	+4%	108/120	0.0441	
	20.2±0.5	24	+10%	120/150	0.0069	
hif-1(ia4) /*smf-3* RNAi	23.7±0.5	28	+1%	101/150	0.7409	Fig. 5G
	22.1±0.5	25	-6%	115/120	0.5484	
	21.0±0.5	24	-11%	109/150	0.3539	
hif-1(ia4) /*ftn-1*/*ftn-2* RNAi	24.3±0.5	28	+4%	119/150	0.117	Fig. 5H
	23.4±0.5	28	0%	111/125	0.1785	
	22.0±0.5	27	-6%	113/150	0.013	
isp-1(qm150) /control RNAi	30.2±0.9	38	+33%	113/150	<0.0001	Fig. 5C, 5D, 5E, 5F
	26.6±0.8	34	+22%	120/150	<0.0001	
	26.5±0.8	33	+44%	144/150	<0.0001	
isp-1(qm150) /*smf-3* RNAi	24.2±0.8	30	-20%	114/120	<0.0001	Fig. 5C
	21.3±0.6	27	-20%	138/150	<0.0001	
	22.0±0.7	29	-17%	142/151	<0.0001	
isp-1(qm150)	27.1±0.8	35	-10%	130/150	0.0045	Fig. 5E

/*ftn-1*/*ftn-2* RNAi						
	23.6±0.7	30	-11%	139/150	0.0013	
	24.0±0.7	31	-9%	148/150	0.041	
isp-1(qm150); hif-1(ia4) /control RNAi	20.9±0.6	24	-31%	141/151	<0.0001	Fig. 5D, 5F
	20.8±0.6	26	-22%	151/153	<0.0001	
	21.5±0.6	26	-19%	142/151	<0.0001	
isp-1(qm150); hif-1(ia4) /*smf-3* RNAi	19.6±0.6	24	-6%	99/120	0.0842	Fig. 5D
	19.5±0.6	23	-6%	129/150	0.0595	
	21.3±0.6	28	-1%	147/150	0.5485	
isp-1(qm150); hif-1(ia4) /*ftn-1*/*ftn-2* RNAi	27.3±1.0	35	+31%	84/90	<0.0001	Fig. 5F
	22.8±0.6	30	+10%	145/150	0.0185	
	25.4±0.7	30	+18%	145/151	<0.0001	

Within this table, the lifespan data sets shaded in the same colors (white or grey) were done in parallel and statistical analysis (p-values) was done within the data set.

$^{\Delta}$: % change in lifespan was calculated against the same control data. Increased (+) or decreased (-) mean lifespan was indicated.

Table S5. Analysis of lifespan and pathogen resistance of *isp-1* mutants.

A. Lifespan analysis of *isp-1* mutants or paraquat treated condition

Strain/treatment	Mean lifespan ±SEM (days)	75th percentile	% change$^{\Delta}$	Number of animals that died/total	p-value vs. control	Figure in text
WT/live *E. coli*	22.5±0.6	26		59/75		Fig. 6D
	18.8±0.5	22		73/100		
WT/dead *E. coli*	31.2±0.9	35	+39%	43/50	<0.0001	Fig. 6D
	32.2±1.0	38	+71%	63/73	<0.0001	
isp-1(qm150)	35.4±0.9	39	+57%	70/100	<0.0001	Fig. 6D

/live *E. coli*						
	25.2±1.3	30	+34%	41/50	<0.0001	
isp-1(qm150) /dead *E. coli*	35.0±1.2	41	-1%	60/100	0.4232	Fig. 6D
	22.6±1.4	32	-10%	49/100	0.3739	
WT/*E. coli*	22.3±0.7	27		82/100		Fig. 6E
	20.7±0.7	24		72/100		
WT/*B. subtilis*	28.2±1.0	36	+26%	54/75	<0.0001	Fig. 6E
	26.8±0.8	34	+29%	65/101	<0.0001	
isp-1(qm150) /*E. coli*	31.8±1.4	41	+43%	74/80	<0.0001	Fig. 6E
	25.5±1.0	34	+23%	85/100	<0.0001	
isp-1(qm150) /*B. subtilis*	33.1±1.2	41	+4%	80/80	0.7871	Fig. 6E
	30.2±1.0	38	+18%	86/100	0.0012	
WT/dead *E. coli*	27.3±0.8	32		82/125		Fig. 6F
	28.9±0.8	30		99/125		
WT/dead *E. coli*, 0.25 mM paraquat	21.8±0.7	25	-20%	45/75	<0.0001	Fig. 6F
	20.9±0.5	23	-28%	84/104	<0.0001	
WT/control	15.1±0.4	19		106/120		Fig. 6G
	14.3±0.3	17		104/121		
WT/0.25 mM paraquat	21.0±0.4	23	+39%	101/120	<0.0001	Fig. 6G
	17.8±0.3	21	+25%	98/120	<0.0001	
pmk-1(km25) /control	16.8±0.5	21	+12%	106/120	0.0031	Fig. 6G
	16.4±0.5	21	+15%	107/120	0.0003	
pmk-1(km25) /0.25 mM paraquat	27.3±0.6	31	+62% (+81%$^{\text{WT ctrl}}$)	106/120	<0.0001 (<0.0001$^{\text{WT par}}$)	Fig. 6G
	26.8±0.5	32	+63% (+87%$^{\text{WT ctrl}}$)	94/120	<0.0001 (<0.0001$^{\text{WT par}}$)	

p-values and % changes for single mutants were calculated against the control immediately above. p-values and % changes for mutants fed with specific bacteria were calculated against the mutant fed with control *E. coli*.

$^{\Delta}$: % changes in lifespan were calculated against the same control data. Increased (+) or

decreased (-) mean lifespan was indicated.

$\%^{WT\ ctrl}$: the % change in lifespan compared to wild-type control.

B. Pathogen resistance of *isp-1* mutants against *Pseudomonas aeruginosa* (PA14)

Strain/treatment	Mean lifespan ±SEM (hours)	75th percentile	% change$^{\Delta}$	Number of animals that died/total	p-value vs. control	Figure in text
WT /*E. coli* to PA14	66.3±1.2	78.3		102/133		Fig 6A
	75.2±1.8	89.3		104/120		
	70.6±1.5	85.3		121/150		
	77.3±1.6	70.1		128/150		
	65.7±2.1	76.0		51/75		
	73.5±1.7	83.6		66/90		
α	66.1±1.0	79.2		69/75		
β	68.2±2.2	77.2		54/78		
isp-1(qm150) /*E. coli* to PA14	81.7±2.2	96.5	+23%	131/140	<0.0001	Fig 6A
	70.2±1.9	90.7	-7%	109/120	0.8256	
	99.4±3.0	122.0	+41%	136/151	<0.0001	
	85.5±2.8	83.6	+11%	133/150	0.0702	
	87.1±3.2	100.0	+33%	68/75	<0.0001	
	80.3±2.4	97.4	+9%	74/90	0.4845 ($0.0420^{50\%}$)	
α	74.7±2.5	78.9	+13%	70/75	0.3788 ($0.0012^{50\%}$)	
β	74.7±2.4	81.3	+9%	61/62	0.3618	
WT /*E. coli* to PA14	82.3±2.0	96.7		94/119		Fig. S5
	97.9±2.1	119.4		97/120		
WT /*B. subtilis* to PA14	70.0±1.3	79	-15%	100/120	<0.0001	Fig. S5
	80.3±2.0	84.8	-18%	97/120	<0.0001	
WT /*B. subtilis* to PA14	47.2±0.8	55.8		104/120		Fig. 6B
	57.2±1.2	60.5		79/120		

isp-1(qm150) /*B. subtilis* to PA14	106.0 ±2.0	125.6	+125%	115/120	<0.0001	Fig. 6B
	111.7 ±2.3	126.7	+95%	126/141	<0.0001	

In this table, survival data sets shaded in the same color (white or grey) or marked as α or β were performed in parallel.

p-values marked in the parentheses as 50% is the p-value at 50% survival point calculated by Fisher's exact test using OASIS (15).

C. Pathogen resistance of *isp-1* mutants against *Enterococcus faecalis.*

Strain/treatment	Mean lifespan ±SEM (Days)	75th percentile	% change$^{\Delta}$	Number of animals that died/total	p-value vs. control	Figure in text
WT/*E. faecalis*	4.6±0.2	6		62/80		Fig. 6C
	4.6±0.2	6		72/95		
isp-1(qm150) /*E. faecalis*	7.0±0.5	10	+52%	64/80	0.0001	Fig. 6C
	7.9±0.5	11	+72%	74/100	<0.0001	

Table S6. Pathogen resistance of *isp-1* mutants on hyper-pathogenic *E. coli* food.

Strain/treatment	Mean lifespan ±SEM (days)	75th percentile	% change$^{\Delta}$	Number of animals that died/total	p-value vs. control	Figure in text
WT/BHI OP50	7.3±0.4	10		51/60		Fig 7A
	5.7±0.3	8		49/60		
	7.2±0.3	9		54/60		
	6.3±0.2	8		47/60		Fig. 7B, 7C
isp-1(qm150) /BHI OP50	10.8±0.5	13	+48%	38/44	<0.0001	Fig 7A
	9.4±0.6	13	+65%	59/60	<0.0001	

	10.4±0.4	13	+44%	49/60	<0.0001	
	9.9±0.4	12	+57%	42/60	<0.0001	Fig. 7B, 7C
hif-1(ia4) /BHI OP50	6.4±0.4	9	+12%	57/60	0.0774	
	7.4±0.3	10	+3%	56/60	0.6750	
	7.4±0.2	9	+17%	53/60	0.0007	Fig. 7B
isp-1(qm150); hif-1(ia4) /BHI OP50	9.8±0.3	11	+53%	38/60	<0.0001 (0.1947^{isp1})	
	9.2±0.2	11	+24%	59/60	<0.0001 ($<0.0001^{isp1}$)	
	7.8±0.3	9	+5%	45/60	0.0257 ($<0.0001^{isp1}$)	Fig. 7B
aak-2(ok524) /BHI OP50	7.7±0.3	9	+35%	36/60	0.0001	
	7.5±0.2	9	+4%	52/60	0.9226	
	7.6±0.2	9	+21%	46/60	<0.0001	Fig. 7C
isp-1(qm150); aak-2(ok524) /BHI OP50	7.1±0.5	10	-8%	51/60	0.7079 ($<0.0001^{isp1}$)	
	8.7±0.2	10	+16%	54/60	<0.0001 ($<0.0001^{isp1}$)	
	8.9±0.2	10	+17%	40/60	<0.0001 (0.0019^{isp1})	Fig. 7C
WT/control RNAi to BHI OP50	7.5±0.2	9		76/90		Fig. 7D, 7F
	6.9±0.2	9		79/90		Fig. 7E
isp-1(qm150) /control RNAi to BHI OP50	9.1±0.4	14	+23%	92/105	0.0001	Fig. 7D, 7F
	8.7±0.4	12	+26%	79/105	<0.0001	Fig. 7E
WT/*dve-1* RNAi to BHI OP50	3.5±0.2	4	-53%	76/90	<0.0001	Fig. 7D
	3.4±0.2	5	-51%	95/90	<0.0001	
isp-1(qm150) /*dve-1* RNAi to BHI OP50	7.1±0.2	9	+101% ($-22\%^{isp1/ctrl}$)	89/105	<0.0001 ($<0.0001^{isp1/ctrl}$)	Fig. 7D
	6.2±0.2	8	+83% ($-32\%^{isp1/ctrl}$)	81/105	<0.0001 ($<0.0001^{isp1/ctrl}$)	
WT/*ubl-5* RNAi to BHI OP50	7.1±0.3	9	-5%	66/90	0.6379	
	6.0±0.3	9	-12%	98/90	0.1254	Fig. 7E

isp-1(qm150) /*ubl-5* RNAi to BHI OP50	10.0±0.5	14	+42% (+10%$^{isp1/ctrl}$)	93/105	<0.0001 (0.1331$^{isp1/ctrl}$)	
	9.6±0.4	13	+60% (+5%$^{isp1/ctrl}$)	99/105	<0.0001 (0.0601$^{isp1/ctrl}$)	Fig. 7E
WT/*ceh-23* RNAi to BHI OP50	7.4±0.2	9	-1%	71/90	0.6739	Fig. 7F
	6.6±0.2	9	-3%	78/90	0.8581	
isp-1(qm150) /*ceh-23* RNAi to BHI OP50	8.3±0.5	12	+12% (-9%$^{isp1/ctrl}$)	66/70	0.0207 (0.3811$^{isp1/ctrl}$)	Fig. 7F
	7.6±0.5	12	+14% (-17%$^{isp1/ctrl}$)	74/105	0.0013 (0.0984$^{isp1/ctrl}$)	
WT/*daf-16* RNAi to BHI OP50	7.1±0.2	9		54/60		
	5.9±0.2	8		43/60		
	5.5±0.3	7		41/60		Fig. S6
	5.4±0.2	7		69/80		
hif-1(ia4) /*daf-16* RNAi to BHI OP50	7.7±0.3	9	+8%	58/62	0.0017	
	5.9±0.2	7	0%	45/60	0.8066	
	5.1±0.3	7	-7%	44/60	0.6407	Fig. S6
	4.9±0.2	6	-9%	70/80	0.1003	

p-values were calculated for single mutants against wild type and for double mutants against the single mutants immediately above.

BHI OP50: hyper-pathogenic OP50 *E. coli* bacteria by culturing in BHI media

p-values in the parentheses were calculated against *isp-1* mutants (^{isp1}) or *isp-1* mutants treated with control RNAi ($^{isp1/ctrl}$).

Dataset S1. Analysis of list of genes that were differently regulated in *isp-1* and *isp-1; hif-1* (q<0.05). Detailed gene lists obtained by comparing with previous microarray data and Mountain analysis (please see the separate spreadsheet file).

SI Materials and Methods

Strains. The following strains were analyzed in this study: N2 wild type, CF2725 *aak-2(ok524) X*, CF2354 *clk-1(qm30) III*, CF2172 *isp-1(qm150) IV*, CF2479 *daf-12(rh61rh411) X*, CF2495 *hsf-1(sy441) I*, CF2732 *sir-2.1(ok434) IV*, IJ6 *hif-1(ia4) V*, IJ7 *vhl-1(ok161) X*, IJ110 *clk-1(qm30)III; iaIs28[P-hif-1::hif-1a::tag + unc-119(+)]*, IJ117 *isp-1(qm150) IV; iaIs28[P-hif-1::hif-1a::tag + unc-119(+)]*, IJ113 *aak-2(rr48) X*, IJ130 *pmk-1(km25) IV*, IJ138 *hif-1(ia4) V; aak-2(ok524) X*, IJ153 *aak-2(ok524) X; iaIs28[P-hif-1::hif-1a::tag + unc-119(+)]*, IJ159 *iaIs28[P-hif-1::hif-1a::tag + unc-119(+)]*, IJ167 *vhl-1(ok161) X; iaIs28[P-hif-1::hif-1a::tag + unc-119(+)]*, IJ 259 *isp-1(qm150) IV; aak-2(ok524) X*, IJ333 *isp-1(qm150) IV; hif-1(ia4) V*, IJ339 *par-4(tm2986) V*, IJ372 *aakb-2(rr88) III*, EU1 *skn-1(zu67) IV/nT1[unc-?(n754) let-?]*, WBM59 *uthIs272[Pmyo-2::tdTOMATO, unc-54 3'UTR]*, WBM60 *uthIs248[Paak-2::aak-2 genomic (aa1-321)::GFP ::unc-54 3'UTR, Pmyo-2::tdTOMATO]*, IJ599 WMB59 outcrossed 4 times with Lee lab N2, IJ600 WBM60 outcrossed 4 times with Lee lab N2

Paraquat treatment. Paraquat stock solution was added onto OP50 *E. coli*-seeded plates directly to achieve a desired concentration. Gravid day 1 adult animals were transferred onto the paraquat-treated plates and removed after 16 hours for synchronization, and the progeny were used for experiments. Because worms arrest as early larvae under high concentrations (1 or 4 mM) of paraquat, L4 stage animals were transferred onto these high concentrations of paraquat-treated plates.

Lifespan analysis. Lifespan assays were performed as described previously (12). Synchronized worms were grown on NGM plates seeded with *E. coli* with or without adding 0.25 mM paraquat at 20℃ until they reached adulthood. Pre-fertile day 1 adults were transferred onto new *E. coli*-

seeded NGM plates treated with 5 μM 5-fluoro-2'-deoxyuridine (FUDR, Sigma St Louis, MO, USA). For the lifespan under various concentrations of paraquat-treated conditions, L4 animals were transferred onto *E. coli*-seeded NGM plates treated with paraquat (0.015, 0.062, 0.25, 0.5, 1, 2, and 4 mM) and FUDR. To prepare plates seeded with dead *E. coli*, streptomycin-resistant overnight cultured OP50 bacteria were pelleted, resuspended, and concentrated (50X) with M9 buffer. Ten μg/ml streptomycin or kanamycin was added to the resuspended *E. coli* and empty NGM plates for preparing live or dead bacteria, respectively. The resuspended *E. coli* solution was seeded on NGM plates and dried overnight and treated with FUDR. For the lifespan assay without FUDR, adult animals were transferred to freshly prepared plates for every other day until the worms produced no progeny. *Bacillus subtilis* (CU1065) was cultured in liquid LB media for 8 hours in a shaking incubator at 37˚C, seeded on NGM plates, and cultured at 37˚C for another 12 hours. Worms were synchronized by bleaching gravid adults using hypochloride solution and the collected eggs were transferred to *B. subtilis*-seeded plates in order to prevent *E. coli* contamination. Note that *B. subtilis* seeded on NG (nematode growth) media quickly form metabolically dormant spores (16). Thus, under our experimental conditions, it is unlikely that the metabolites of *B. subtilis* affected lifespan results, as shown in a previous study (16). Worms were scored as live or dead for every two or three days until all the worms were dead. Animals that were ruptured, displayed internal progeny hatching, burrowed or crawled off the plates were censored as described previously (12).

RNA interference. *E. coli* feeding RNAi clones targeting *smf-3*, *ceh-23*, and *dve-1* were cultured from the Ahringer *C. elegans* RNAi library. *ftn-1* and *ftn-2* RNAi clones were from the *C. elegans* ORFeome RNAi library. Empty vector (L4440) was used as a control. Genomic DNA of

ubl-5 (898 bp) was cloned into L4440 vector and transformed into HT115 *E. coli*. Each RNAi clone was cultured overnight in LB broth containing 50 μg/ml ampicillin (USB, Santa Clara, CA, USA). For *ftn-1*/*ftn-2* (mixed in equal volume) and *smf-3* RNAi, the optical density at 590 nm values of overnight cultured *E. coli* were adjusted to 0.9 (17). RNAi bacteria were spotted on NGM plates containing ampicillin (50 μg/ml), and cultured overnight at 37˚C. To induce double-stranded RNAs, 1 mM isopropyl β-D-1-thiogalactopyranoside (IPTG, GOLDBIO, St. Louis, MO, USA) was added on the plates before usage.

Western blot analysis. Synchronized worms that reached mid-L4 stage were used to measure phosphorylated AAK-2 in **Figures 1G** and **2G**. Synchronized L4 to young adult worms were used to detect HIF-1::myc levels in **Figures 2A** and **2C**. In **Figure S2D**, L4 to young adult worms cultured on control RNAi plates were harvested, transferred, and cultured on control or *daf-15* RNAi-seeded plates treated with FUDR for 3 days and harvested. To obtain sufficient amount of worm samples, we used mixed staged worms (mostly late larvae and young adults) for *clk-1* and *isp-1* mutants, and wild-type animals in **Figures 1H** and **2B**. Animals were harvested and washed twice by using M9 buffer, and subsequently centrifugated at 5,000 rpm briefly. The worm pellets were immediately frozen using liquid nitrogen, mixed with SDS sample loading buffer (2X), and boiled for 10 minutes. Worms were further broken by vortexing for 10 minutes, and then centrifuged for 30 minutes at 13,000 rpm to eliminate insoluble debris. The worm lysates were electrophoresed using 8% SDS-PAGE and transferred to PVDF membrane. The PVDF membrane was blocked with 5% skim milk or 5% BSA in PBS-T (0.1% Tween 20) or TBS-T(0.1% Tween 20), and subsequently incubated with primary antibodies against c-myc (# sc-40 Santa Cruz, Santa Cruz, California, USA 1:1000) or phospho-AMPKα (#4188 Cell

Signaling Beverly, MA, USA 1:2000). Anti-mouse (1:10,000) or anti-rabbit (1:15,000) secondary antibodies conjugated with horseradish peroxidase were used for anti c-myc or anti phospho-AMPKα primary antibodies, respectively. The PVDF membrane was incubated in the chemoluminescent horseradish peroxidase substrate (Thermo Rockford, IL, USA) for 1 minute, and the signal was detected by using X-ray film (Agfa).

GST-HIF-1 fusion protein purification. HIF-1N (aa 1-365) and HIF-1C (aa 359-719) terminal protein regions were cloned into pET-49b(+) and transformed into BL21* competent cells (Invitrogen). Site-directed mutagenesis to generate S419A and S551A mutant clones was performed by following the Site-Directed Mutagenesis manual (Stratagene). For the recombinant protein induction, 0.7 mM IPTG was added to the LB broth. GST-HIF-1C was induced at 37˚C for 3 hours, whereas GST-HIF-1N was induced at 18˚C for 24 hours because of insolubility at 37˚C. Harvested *E. coli* were resuspended in lysis buffer (50 mM Tris-HCl pH 7.4, 150 mM NaCl, 1% Triton X-100, 1 mM DTT, 1 mM PMSF, 0.1 μM aprotinin, 1 mM benzamidine, and 1 μg/ml leupeptin), sonicated, and centrifuged at 13,000 rpm, 4˚C for 20 minutes. The protein supernatant was incubated with Glutathione Sepharose 4B (GE healthcare) for 3 hours at 4˚C. Protein bound Glutathione Sepharose was washed with lysis buffer for 8 times to reduce non-specifically bound proteins.

***In vitro* AMPK kinase assay.** *In vitro* AMPK kinase assay was performed as previously reported with some modifications (18). Purified recombinant human AMPK (171539, Merck Millipore, Billerica, MA) was prepared according to the manufacture's instruction. In total of 25 μl reaction volume, resin bound substrates (1~2 μg) were incubated with 2 μl of AMPK, 5 μl of kinase reaction buffer (25 mM MOPS, 25 mM $MgCl_2$, 12.5 β-glycerophosphate, 5 mM EGTA, 2 mM

EDTA pH 7.2, 0.25 mM DTT), 5 µl of final 125 µM ATP, 2 µCi radiolabeled ATP with or without 5 µl of final 150 µM AMP at 30˚C for 10 minutes. SDS sample loading buffer (5X) was added to terminate the reaction, and the samples were boiled at 95˚C for 10 minutes. Each sample was loaded on an 8% SDS-page gel, stained with Coomassie brilliant blue, and heat dried. ^{32}P signals were detected by a phosphorimager (Fuji Film FLA-2000). To identify HIF-1 phosphorylation residues, phosphorylated GST-HIF-1C was excised from the gel for in-gel digestion and analysed by LC-MS/MS.

In-gel digestion. In-gel digestion and LC–MS/MS analysis were done following the steps described previously (19). The gel band was cut into approximately 1 mm cubes, and washed with distilled water. Subsequently the gel pieces were destained using 25 mM NH_4HCO_3 in 50% CH_3CN, dehydrated with 100% CH_3CN and dried in air at room temperature (25^{o}C). The dried gel pieces were reduced with 10 mM dithiothreitol (DTT) at 56^{o}C for 1 hour followed by alkylated with 55 mM iodoacetamide for 1 hour in the dark at room temperature (25^{o}C). Washing with 25 mM NH_4HCO_3 in 50% CH_3CN, the gel pieces were again dehydrated with 100% CH_3CN and dried in air at room temperature (25^{o}C). For trypsin digestion, pre-cooled dry gel pieces were rehydrated with 12.5 ng/µl trypsin (in 25 mM NH_4HCO_3) on ice for 30–45 minutes. Excess trypsin was washed with 25 mM NH_4HCO_3, and digestion was carried out overnight at 37^{o}C. Digests were extracted once with 25 mM NH_4HCO_3 in 50% CH_3CN, once with 0.2% trifluoroacetic acid (TFA) in 50% CH_3CN, and finally once with 0.2% TFA in 70% CH_3CN. The eluted sample was dried completely under vacuum, and stored at −20^{o}C until use.

LC-MS/MS analysis. Peptide samples were reconstituted with 0.4% acetic acid and was injected from a cooled (10^{o}C) auto sampler into a reversed-phase Magic C18aq (Michrom BioResources,

Auburn, CA) column (15 cm×75 μm, packed in-house) on an Eksigent nanoLC-ultra 1D plus system at a flow rate of 300 nL/min. Prior to use, the column was equilibrated with 95% buffer A (0.1% formic acid in H_2O) and 5% buffer B (0.1% formic acid in acetonitrile). The peptides were eluted with a linear gradient from 5% to 30% buffer B over 30 minutes and 30% to 50% buffer B over 8 minutes followed by an organic wash and aqueous re-equilibration at a flow rate of 300 nL/min with a total run time of 75 minutes. The HPLC system was coupled to a Q Exactive quadrupole mass spectrometer (Thermo Scientific, Bremen, Germany) operated in the data-dependent mode. Survey full-scan MS spectra (m/z 300–2000) were acquired with a resolution of 75000. Source ionization parameters were as follows: spray voltage, 1.9 kV; capillary temperature, 275^{o}C; and s-lens level, 44.0. The MS/MS spectra of the 12 most intense ions from the MS1 scan with a charge state≥2 were acquired with the following options: resolution, 17500; isolation width, 2.0 m/z; normalized collision energy, 27%; dynamic exclusion duration, 30 s; and ion selection threshold, 4.00E+03 counts.

Database search and data process. The raw data were searched using Sequest algorithm in Proteome Discoverer 1.4 (Thermo Scientific Inc., San Jose, CA). The method outline used in the spectrum selector node of the Proteome Discoverer software included the following scan event filters: fragmentation method, ionization source, and Unrecognized Activation Type Replacements parameters and all were set to default settings to generate MS/MS spectra. Retention time, precursor charge state (high/low), total intensity threshold value, minimum peak count was set to default settings. The Min and Max precursor mass settings were 350 and 5000 Da, respectively. The database search included *C. elegans* HIF-1 C terminus GST protein and the common contaminants. The search parameters included in this study were: full tryptic peptide

cleavage specificity, two missed cleavages, fixed modification of carbamidomethyl cysteine (+57.021 Da), and variable modifications of oxidized methionine (+15.995 Da), phosphorylated Ser, Thr, and Tyr (+79.9799). The Sequest algorithm parameters were: Dta generation threshold =10000, precursor ion mass tolerance =15 ppm, fragment ion mass tolerance for ion trap MS/MS was 0.05 Da. The criteria used for acceptance of peptide assignments are as follows: Minimal XCorr value for each charged state ranging from 1 to 7 was 1.50, 2.0, 2.25, 2.75, 3.0, 3.2, and 3.4 respectively. A strict FDR of 0.01 and a relaxed FDR of 0.05, a total of two target values, for a decoy database search were applied.

Quantitative-RT PCR. Quantitative-RT PCR experiments were performed as described previously (12). Synchronized L4 (**Figure 2**) or day 1 young adult worms (**Figure 5**) were used for RNA extraction. RNA was isolated using RNAiso plus (#9109, TaKaRa, Seta, Kyoto, Japan) and reverse transcribed to cDNA using ImProm-II™ Reverse Transcriptase (Promega). Quantitative real time PCR was performed using Step One Real time PCR system (Applied Biosystem) and analyzed using $^{\Delta\Delta}$Ct methods described in the manufacturer's manual. The level of *ama-1* mRNA was used for normalization.

Sequences of primers used for quantitative RT-PCR analysis. *ama-1*-Forward: TGGAACTCTGGAGTCACACC, Reverse: CATCCTCCTTCATTGAACGG; *hif-1*-Forward: CAGTGATTCTTCAATTCTTTACGTC, Reverse: CTGTTAAATCTGTCTGTGTTAATCC; *aak-2*-Forward: CGTGGAACTAGAACGTCAAG; *aak-2*-Reverse: GTCACATCGCACGACATGTC; *ftn-1*-Foward: GTCAATAAACAGATTAACGTAGAAC, *ftn-1*-Reverse: CGAAGTGCGATATCATCACGATCG; *smf-3*-Foward: GCTGTAGTGATCTTCTCCGGC; *smf-3*-Reverse: GAAGTTGAATCAGCTGCAAGC

Measurement of overall ROS levels by using 2',7'-dichlorofluorescein diacetate (DCF-DA). To measure the overall ROS levels, a DCF-DA (Molecular Probes, Carlsbad, CA, USA) assay was used as described previously (12). Briefly, approximately 1000 day 1 young adult worms were collected in M9 buffer and washed three times to eliminate bacteria. For experiments that include paraquat feeding, animals were harvested and fed with fresh *E. coli* for 30 minutes to eliminate ROS produced from paraquat-treated residual *E. coli*. At a high concentration of paraquat (4 mM) a majority of animals died during sample collection, and therefore we were not able to collect sufficient live worms to perform the assay.

Measurement of hydrogen peroxide levels by using Amplex Red assay. Amplex Red assay was performed as describe previously (20) with some modifications. For 0.25 mM paraquat-treated conditions, harvested worms were washed and fed with fresh *E. coli* for 30 minutes to eliminate the hydrogen peroxide production from residual *E. coli* treated with paraquat. Approximately 200~300 day 1 young adults were collected and washed twice with M9 buffer to eliminate bacteria and washed once with 50 mM sodium phosphate (pH 7.4). Fifty μl of the buffer with live worms or standard hydrogen peroxide solutions (2.5 μM to 40 μM) were mixed with 50 μL of Amplex Red working solution (100 μM Amplex® Red reagent with 0.2 U/mL HRP) and incubated for 3 hours at 20˚C. After incubation, the worms were settled down to collect 50 μl of the supernatant, which was used for measuring hydrogen peroxide by applying to a plate reader (ELx800 Absorbance Microplate Reader) at 570 nm. Residual 50 μl of the worm-containing solution was used for the normalization of samples by quantifying tubulin protein levels employing Western blot.

Microarray sample preparation. *isp-1(qm150)* and *isp-1(qm150); hif-1(ia4)* animals were

grown on NGM plates with live OP50 bacteria. Worms were harvested when the majority of the population reached mid-L4 stage. Total RNA was isolated using Tri-reagent (Molecular Research Center, Inc.) and purified with the RNeasy kit (Qiagen). cRNA synthesis/ amplification and Cy3/Cy5 dye labeling, and hybridization onto Agilent 4X44K *C. elegans* oligonucleotide microarrays(v2) were performed as previously described (21). One out of the three arrays was dye-flip replicate.

Micorarray data analysis. Microarray raw data were normalized using Agilent feature extraction software. The normalized data were uploaded onto to the Princeton University MicroArray database (PUMA [http://puma.princeton.edu]). The raw data were retrieved by SUID (Sequence Unique IDentifier) then averaged by Wormbase ID. Log2-transformed fold change was acquired after filtering out genes with <80% good data. For statistical analysis, the set of genes that were consistently up- or down-regulated from all three replicated microarray data set were extracted by using the Python programming language and R package. The p-values were estimated using Student's *t*-test. The q-values represent the probability of seeing the observed number of genes that would be significant in all replicated microarray data sets (22, 23). The q-values for each test to correct the multiple testing errors were calculated by using the R package (24) and the cutoff used in this analysis was $q<0.05$ (after Bonferroni correction).

Pathogen resistance analysis. Pathogen resistance against PA14 was measured as described previously (25). Briefly, high peptone (0.35%) NGM plates were prepared by seeding 5 μl overnight culture of PA14. Worms were synchronized and grown until L4 or young adults on OP50-seeded NGM plates at 20℃. These L4 or young adult worms were transferred onto PA14 plates treated with 5 μM FUDR and kept in a 25℃ incubator. Animals were examined for every

6~12 hours and scored as alive if they moved when prodded. Resistance assay against *E. faecalis* was performed as previously described without FUDR treatment, since FUDR treatment reduced the pathogenicity of *E. faecalis* (26). Survival analysis on pathogenic *E. coli* was performed as previously described (26). Briefly, a single colony of OP50 was cultured in brain heart infusion (BHI) media and incubated for 3~4 hours at 37℃, spotted on solid (2% agar) BHI plates, and incubated overnight at 37℃. Plates were examined at ~24 hour interval for *E. faecalis* and BHI medium-cultured OP50 to examine the survival of animals. For RNAi experiment, *E. coli* expressing *dve-1*, *ubl-5* or *ceh-23* double stranded RNA (dsRNA) was cultured, spotted on NG plates containing ampicillin, and incubated overnight at 37℃. IPTG (1 mM) was added for the induction of dsRNA and L4 or young adult animals grown on these plates were transferred to BHI medium-cultured OP50 plates to examine the survival. The survival data were analyzed by using OASIS (online application for the survival analysis of lifespan assays http://sbi.postech.ac.kr/oasis/surv/) (15).

Supporting References

1. Yang W & Hekimi S (2010) A mitochondrial superoxide signal triggers increased longevity in *Caenorhabditis elegans*. *PLoS Biol* 8(12):e1000556.
2. Shackelford DB & Shaw RJ (2009) The LKB1-AMPK pathway: metabolism and growth control in tumour suppression. *Nature reviews. Cancer* 9(8):563-575.
3. Shackelford DB, *et al.* (2009) mTOR and HIF-1a-mediated tumor metabolism in an LKB1 mouse model of Peutz-Jeghers syndrome. *Proceedings of the National Academy of Sciences of the United States of America* 106(27):11137-11142.

4. Shen C, Nettleton D, Jiang M, Kim SK, & Powell-Coffman JA (2005) Roles of the HIF-1 hypoxia-inducible factor during hypoxia response in *Caenorhabditis elegans*. *The Journal of biological chemistry* 280(21):20580-20588.

5. Bishop T, *et al.* (2004) Genetic analysis of pathways regulated by the von Hippel-Lindau tumor suppressor in *Caenorhabditis elegans*. *PLoS Biol* 2(10):e289.

6. Curtis R, O'Connor G, & DiStefano PS (2006) Aging networks in *Caenorhabditis elegans*: AMP-activated protein kinase (*aak-2*) links multiple aging and metabolism pathways. *Aging cell* 5(2):119-126.

7. Xie M & Roy R (2012) Increased levels of hydrogen peroxide induce a HIF-1-dependent modification of lipid metabolism in AMPK compromised *C. elegans* dauer larvae. *Cell metabolism* 16(3):322-335.

8. Zarse K, *et al.* (2012) Impaired insulin/IGF1 signaling extends life span by promoting mitochondrial L-proline catabolism to induce a transient ROS signal. *Cell metabolism* 15(4):451-465.

9. Honda Y & Honda S (1999) The *daf-2* gene network for longevity regulates oxidative stress resistance and Mn-superoxide dismutase gene expression in *Caenorhabditis elegans*. *FASEB journal : official publication of the Federation of American Societies for Experimental Biology* 13(11):1385-1393.

10. McElwee J, Bubb K, & Thomas JH (2003) Transcriptional outputs of the *Caenorhabditis elegans* forkhead protein DAF-16. *Aging cell* 2(6):111–121.

11. Murphy CT, *et al.* (2003) Genes that act downstream of DAF-16 to influence the lifespan of *Caenorhabditis elegans*. *Nature* 424(6946):277-283.

12. Lee SJ, Hwang AB, & Kenyon C (2010) Inhibition of respiration extends *C. elegans* life

span via reactive oxygen species that increase HIF-1 activity. *Curr Biol* 20(23):2131-2136.

13. Apfeld J, O'Connor G, McDonagh T, DiStefano PS, & Curtis R (2004) The AMP-activated protein kinase AAK-2 links energy levels and insulin-like signals to lifespan in *C. elegans*. *Genes Dev* 18(24):3004-3009.

14. Leiser SF, Begun A, & Kaeberlein M (2011) HIF-1 modulates longevity and healthspan in a temperature-dependent manner. *Aging cell* 10(2):318-326.

15. Yang JS, *et al.* (2011) OASIS: online application for the survival analysis of lifespan assays performed in aging research. *PLoS One* 6(8):e23525.

16. Gusarov I, *et al.* (2013) Bacterial nitric oxide extends the lifespan of *C. elegans*. *Cell* 152(4):818-830.

17. Rea SL, Ventura N, & Johnson TE (2007) Relationship between mitochondrial electron transport chain dysfunction, development, and life extension in *Caenorhabditis elegans*. *PLoS Biol* 5(10):e259.

18. Mair W, *et al.* (2011) Lifespan extension induced by AMPK and calcineurin is mediated by CRTC-1 and CREB. *Nature* 470(7334):404-408.

19. Kabir MH, Suh EJ, & Lee C (2012) Comparative phosphoproteome analysis reveals more ERK activation in MDA-MB-231 than in MCF-7. *Int J Mass Spectrom* 309:1-12.

20. Chavez V, Mohri-Shiomi A, Maadani A, Vega LA, & Garsin DA (2007) Oxidative stress enzymes are required for DAF-16-mediated immunity due to generation of reactive oxygen species by *Caenorhabditis elegans*. *Genetics* 176(3):1567-1577.

21. Shaw WM, Luo S, Landis J, Ashraf J, & Murphy CT (2007) The *C. elegans* TGF-beta Dauer pathway regulates longevity via insulin signaling. *Curr Biol* 17(19):1635-1645.

22. Jung K, Friede T, & Beissbarth T (2011) Reporting FDR analogous confidence intervals for the log fold change of differentially expressed genes. *Bmc Bioinformatics* 12.

23. McCarthy DJ & Smyth GK (2009) Testing significance relative to a fold-change threshold is a TREAT. *Bioinformatics* 25(6):765-771.

24. Storey JD & Tibshirani R (2003) Statistical significance for genomewide studies. *Proceedings of the National Academy of Sciences of the United States of America* 100(16):9440-9445.

25. Tan MW, Mahajan-Miklos S, & Ausubel FM (1999) Killing of *Caenorhabditis elegans* by *Pseudomonas aeruginosa* used to model mammalian bacterial pathogenesis. *Proceedings of the National Academy of Sciences of the United States of America* 96(2):715-720.

26. Garsin DA, *et al.* (2001) A simple model host for identifying Gram-positive virulence factors. *Proceedings of the National Academy of Sciences of the United States of America* 98(19):10892-10897.